# Fluid-induced instabilities of rotors:
## Whirl and whip - summary of results

*by Agnes Muszynska, PhD.*
*Senior Research Scientist Bently Rotor Dynamics Research Corporation*

*and Donald E. Bently*
*Chairman and Chief Executive Officer Bently Nevada Corporation*
*President, Bently Rotor Dynamics Research Corporation*

**Notation**

| | |
|---|---|
| $A_1$, $A_2$ | Amplitudes of rotor self-excited vibrations |
| c | Bearing radial clearance |
| D | Fluid film radial damping |
| $D_s$, M | Rotor modal damping and mass, respectively |
| F, $F_r$ | Fluid film force in stationary and rotating coordinates, respectively (coordinates rotate at angular velocity $\lambda\Omega$) |
| $j = \sqrt{-1}$ | |
| $K_0$, $K_B$ | Linear and nonlinear parts of the fluid film radial stiffness |
| $K_1$,$K_2$,$K_3$ | Rotor partial model stiffnesses of rotor/seal model (for rotor/bearing model is the supporting spring stiffness) |
| $M_f$ | Fluid film inertia effect |
| s | Eigenvalue |
| t | Time |
| x,y,$x_r$,$y_r$ | Rotor lateral orthogonal displacements in stationary and rotating coordinates, respectively (coordinates rotate at angular velocity $\lambda\Omega$) |
| r=x+jy | Rotor lateral displacement in stationary coordinates |
| $r_r=x_r+jy_r$ | Rotor lateral displacement in rotating coordinates |
| $r_1$,$r_2$ | Rotor lateral displacements at the disk and bearing, respectively |
| $\alpha$ | Phase difference between bearing and disk self-excited vibrations |
| $\lambda$ | Fluid circumferential average velocity ratio |
| $\omega$ | Complex eigenvalue. Also rotor self-excited vibration frequency. |
| $\omega_n$ | Rotor bending mode natural frequency |
| $\Omega$ | Rotative speed |

This article summarizes laboratory results from experiments conducted on a rotor model. These experiments proved that a model of fluid dynamic forces acting on a concentric, or slightly eccentric, elastically-supported cylinder rotating in a stationary cylinder can adequately predict the system natural frequencies of the first and higher modes, instability thresholds and the existence of self-excited vibrations. Self-excited vibrations, which are also known as whirl or whip, occurred, due to interaction with the surrounding fluid. This article also discusses the physical factors that affect fluid whirl and whip.

### Introduction

The dynamic characteristics of most fluid-handling machine rotors depend on physical phenomena taking place in rotor-surrounding fluids. In particular, the phenomena occur in interstage seals, blade-tip clearances and fluid-lubricated bearings. In all these cases, a description of the physical situation can be simplified as a cylinder rotating inside a stationary cylinder, with a relatively small clearance between them. Independently from the axial component of the flow inside the clearance, the rotating cylinder (rotor) forces the fluid, through viscous friction, to rotate, creating a circumferential flow. The rotating fluid begins to participate in the system dynamics. New forces are generated in the fluid film, which, in a feedback loop, act on the rotor. The rotor responds with lateral vibrations, resulting in a forward, almost circular precession, known as "fluid whirl" and "whip" [1].

The description of fluid whirl and whip that follows is based on the example of a flexible rotor supported by a laterally rigid pivoting brass oilite bearing at the inboard end, and by a 360 oil-lubricated bearing at the outboard end. In order to set the rotor journal at any radial position inside the outboard bearing clearance, adjustable radial supporting springs were attached to the rotor through a rolling element bearing (Figure 1). The concentric journal position was chosen as the first step, because it creates the most favorable conditions for a fluid-induced instability to occur.

### Fluid whirl and whip

Rotor lateral vibrations are measured by two sets of XY proximity probes (Figure 2). Data in the upper plot is from

probes mounted at rotor midspan; data in the lower plot is from probes mounted at the fluid-lubricated bearing. Each full spectrum cascade plot includes Plus Orbit plots, which show the magnified actual paths of the rotor centerline at various rotative speeds. At low rotative speed, the only lateral vibration component in the spectrum is synchronous 1X vibration, due to an unbalance in the rotor (Figure 2). The rotor unbalance acts as a centrifugal rotating force which excites rotor 1X responses. A new vibration component appears in the spectrum at the rotative speed known as the instability threshold (onset). On machines, such as the one considered, it occurs at a speed that is usually lower than the machine's nameplate first balance resonance (critical). At the threshold of instability, the rotor motion becomes unstable, and the lateral vibration amplitudes start increasing. At first, this growth is almost instantaneous. Then it slows down, due to the nonlinear effects in the fluid film at higher eccentricity. In a few rotations, a new state of equilibrium is achieved. This new component in the rotor vibrational response spectrum is the *limit cycle of self-excited vibrations*, known as *fluid whirl*, or in this case, *oil whirl*. The frequency of fluid whirl is lower than rotative speed, $\Omega$ , and, for the considered system is 0.475 $\Omega$ (in general, it can be any fraction, $\lambda$). The important characteristic of the fluid whirl is that its frequency is proportional to the rotative speed. This proportionality can be observed on the spectrum cascade plots (Figure 2) between 2400 to 2600 rpm and 4300 to 6000 rpm.

During fluid whirl, the mode of rotor vibration is conical, like a rigid body. The journal orbits are circular, and forward. When the rotative speed approaches the machine's first balance resonance, (the rotor lateral mode first natural frequency), the 1X vibration amplitudes start increasing. The rotating unbalance force pushes the journal to the side of the bearing, resulting in high dynamic eccentricity. This action causes the flow pattern to change and the fluid film radial stiffness to increase. This action results in a temporary suppression of the fluid whirl [2], changing the flow pattern, and increasing the fluid film radial stiffness [2]. The cessation of the fluid whirl follows. In this case, the unbalance force acts similar to a radial constant force (such as gravity, for instance), which causes the journal to move to a higher eccentricity. This modification of the flow pattern, and increase of the radial stiffness, stabilizes the rotor. The fluid whirl ceases. In contrast to a unilateral radial force, the unbalance force acts in a rotational fashion, not in a constant direction and results in 1X dynamic eccentricity, not a static one. The effects are, however, similar. The rotative speed width of the rotative speed range, where there is no whirl, depends on the amount of rotor unbalance. For a balanced rotor, it is reduced to zero.

It is important to note that the mechanical resonance frequency is not constant; it changes as a function of the journal eccentricity ratio. At a low eccentricity ratio, where the journal is located near the center of the clearance, the fluid film radial stiffness and mechanical resonance frequency are lower. At a high eccentricity ratio, where the shaft is positioned near the periphery of the clearance, the fluid film radial stiffness and, therefore, the mechanical resonance frequency are higher. As a matter of fact, this resonance frequency corresponds to the case of a rigidly-supported rotor. The high "eccentricity" resonance frequency is typically the manufacturer's "nameplate critical." The fluid-induced resonance frequency is also not constant: it changes as a function of the eccentricity ratio. At a high eccentricity ratio, the fluid average circumferential velocity ratio $\lambda$ is low and the fluid-induced resonance frequency is lower. At a low eccentricity ratio, the fluid average circumferential velocity ratio ($\lambda$) is high and the fluid-induced resonance frequency is higher.

When continuing the rotative speed increase, after the first balance resonance, 1X amplitudes decrease, the forced dynamic eccentricity of the journal is reduced, flow pattern

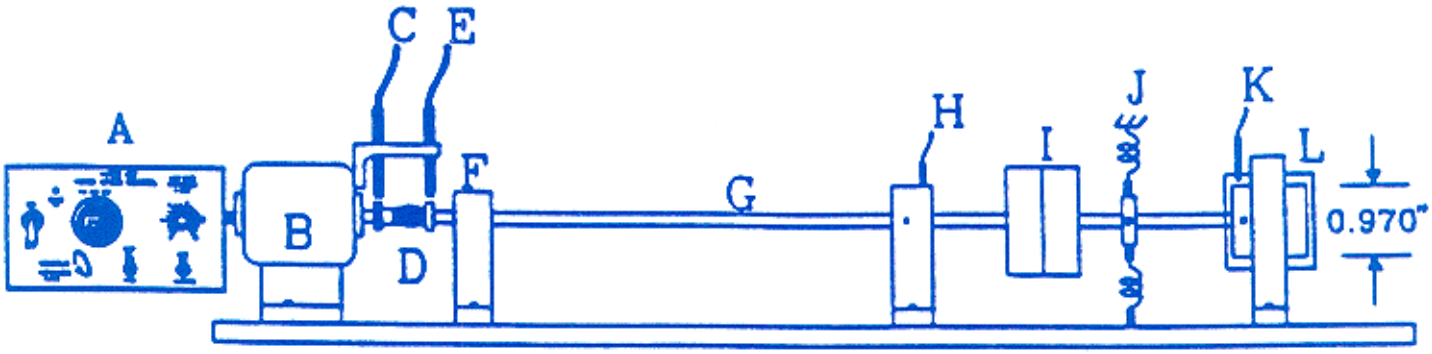


**Figure 1**

**Rotor/bearing system. A - speed controller, B - 75 W electric motor, C - speed controller transducer, D = elastic coupling, E - Keyphasor® (once per turn) transducer, F - laterally rigid, pivoting bearing, G - 9.5 mm (0.375 in) diameter steel shaft, H, K - four proximity eddy current transducers, mounted in XY configuration, I - rotor disk of mass 1.63 kg (3.616 lb), J - four radial supporting spring systems, L - oil (T-10) lubricated bearing with 51 mm (2.0 in) length, 22 µm (8.6 mils) radial clearance and two-port supply oil with 10342 Pa (1500 lb/in$^2$) pressure.**

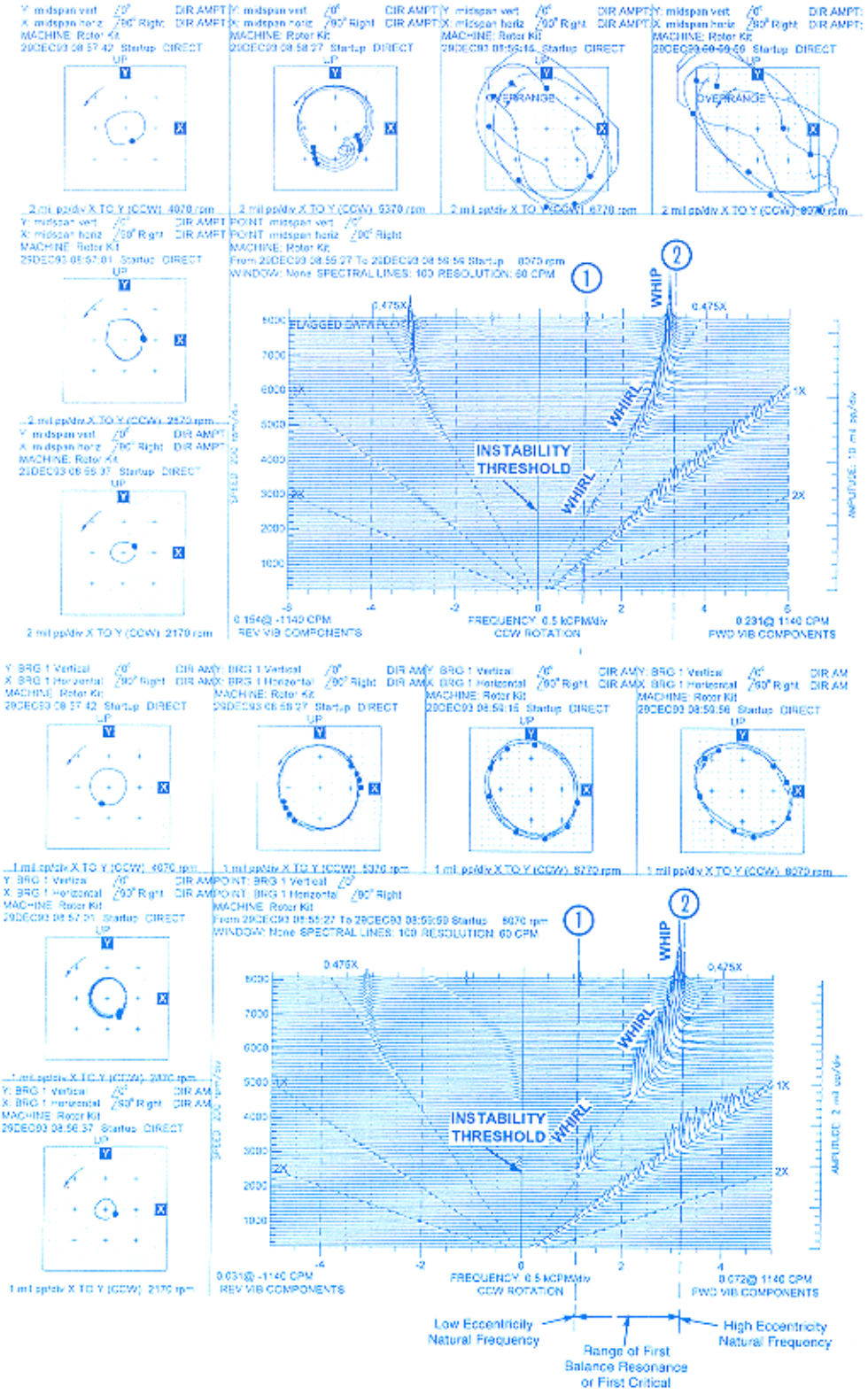


**Figure 2**

**Full spectrum cascade of the rotor midspan (a) and journal (b) lateral vibrations with orbits at different rotative speeds. Using information from two orthogonal transducers, the full spectrum displays forward and reverse circular components of rotor elliptical orbits of all frequency components. The orbits at 5370 rpm show the whirl pattern. Orbits at 6770 and 8070 rpm show the whip pattern.**

goes back to a predominant circumferential flow, and the fluid whirl reoccurs at the *second onset of instability*. The whirl characteristics are similar to those in the lower rotative speed range, maintaining the same proportionality factor of its frequency to the rotative speed. When the rotative speed approaches a value that is approximately twice the first balance resonance, the whirl frequency no longer maintains proportionality to the rotative speed. However, the frequency ratio starts decreasing. (In the considered case, this rotative speed is actually the speed close to the inverse of ($\lambda$) times the first natural frequency, $\omega_n$ , $1/0.475 = 2.11\omega_n$ ).

While the frequency ratio decreases, the whirl amplitudes, especially at the rotor midspan location, significantly increase. With the rotative speed continuing to increase, at the end of this smooth transition, the frequency of the self-excited vibrations asymptotically approaches the constant frequency which corresponds to the rotor high eccentricity first bending mode natural frequency, $\omega_n$ . This *rotor self-excited vibration* is called fluid whip (*oil whip*, in this case). The rotor mode is no longer a conical, rigid body. It is the rotor first bending mode, which is associated with $\omega_n$ . The whip orbits at the journal are circular, forward, and their amplitudes are almost equal to the bearing clearance. At midspan, they are much larger and slightly elliptical, since the rotor system has some residual lateral anisotropy. The unfiltered orbits in Figure 2 show the effect of two major frequency component interactions: The self-excited and the 1X vibrations. The small black dots in the orbits plots are generated by the Keyphasor® transducer, and they indicate the vibration-to-rotation frequency relationship. Two consecutive dots indicate one shaft rotation. Therefore, the whirl orbits of frequency 0.475X will show two dots with the angle between them equal to 0.475 ˜ 360° = 171°. (On the oscilloscope screen set in orbital mode, these two dots will appear to rotate in the direction against rotation, as at each two rotations, they lag the orbit full circle by 360° - 2 x 171° =18°).

Fluid whirl and whip are two variations of the same phenomenon, which is known as the fluid-induced instability of rotors. Two different terms are used because the same phenomenon was discovered independently on two different machines: "whirl" in machines with an operating speed lower than twice the first balance resonance and "whip" in high speed machines with an instability threshold larger than twice first balance resonance. Since whirl and whip were observed independently, nobody, at that time, connected them.

## A new natural frequency of the rotor/bearing system

Fluid whirl and whip are both self-excited vibrations. It is well-known that the self-excited vibrations, as limit cycles of transition from an unstable mode, are conditioned by system nonlinearities. The limit cycle frequencies are, however, weakly sensitive to nonlinearities, and are equal to the natural frequency of the system at the instability onset. There is no doubt about such a relationship in the case of the fluid whip; its frequency corresponds to the rotor high eccentricity natural frequency of the first bending mode or nameplate critical. The following conclusion for fluid whirl is obvious: The whirl frequency, $\lambda\Omega$, must be close to the natural frequency of the rotor/bearing fluid system. In contrast to the classical natural frequencies of mechanical systems, which are based upon stiffness and mass, the whirl natural fre-

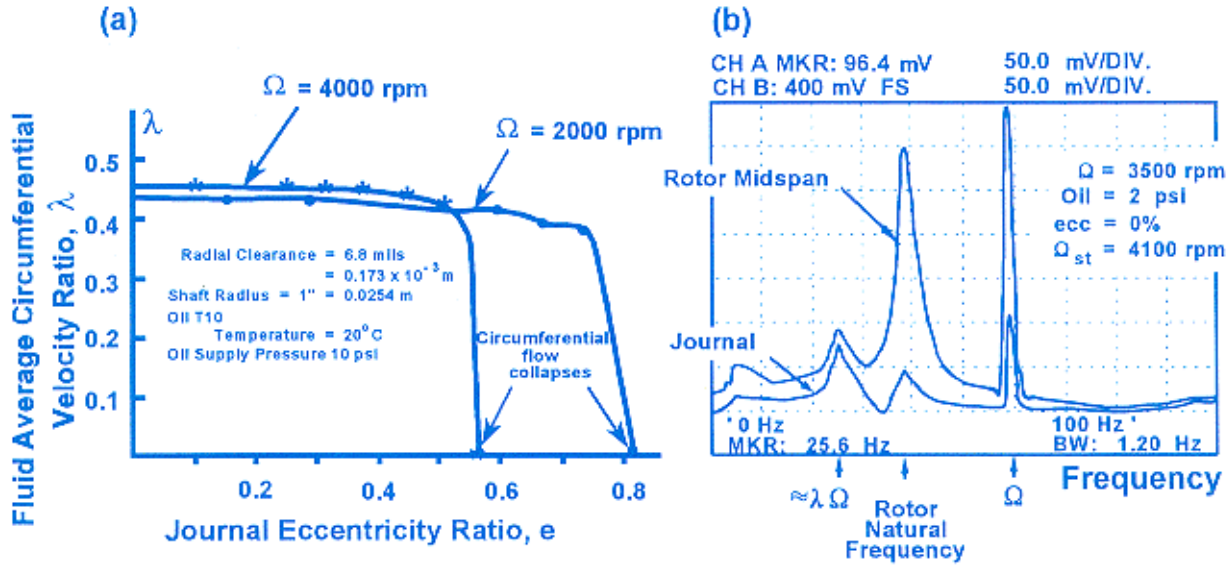


**Figure 3**

**a) An example of fluid circumferential velocity ratio, λ, versus rotor eccentricity ratio e=|r|/c (c = radial clearance) for two values of rotative speeds, obtained from impact testing of an operating rotor/bearing system [7]. (b) Spectrum analyzer screen display during impact testing. Three peaks appear: λΩ, rotor bending mode natural frequency, and the rotative speed frequency, Ω.**

quency is fluid-related, and its dominant characteristic is *viscous damping*. The radial damping in the fluid film has an over-critical value. There is also an important difference in the fluid film damping force, in comparison to classical dashpot damping. In the case of seals and lightly-loaded bearings, the fluid *damping force rotates*. The angular velocity of the fluid damping force rotation is $\lambda\Omega$. This rotation generates an additional, angular velocity-related damping force, which acts on the rotor in the *tangential direction*. This is the driving agent for the fluid whirl and whip.

The analysis of rotor/fluid systems has generated the following important results:

(a) The extension of Modal Analysis to include fluid/solid interaction effects [3-6]

(b) The adjustment of the fluid force models in seals and lightly-loaded bearings [7, 8]

(c) The extension of the fluid force model for other cases, such as blade tip clearance and rotating stall cases [9].

## Model of fluid film forces in seals and lightly-loaded bearings

The fluid force model discussed below can also be applied to seals and lightly-loaded bearings when an almost concentric cylinder rotates inside a stationary cylinder, with a small clearance, and when the dominant fluid flow pattern is rotor rotation and friction-induced circumferential flow. For the concentric "cylinders," the average dynamic force of the fluid film in the radial direction, $F_r$, expressed in the coordinate system $x_r, y_r$, which rotates at the angular velocity $\lambda\Omega$, is as follows [7, 8]:

$$-F_r = M_f \ddot{r}_r + D\dot{r}_r + \left[K_0 + K_B\left(|r_r|\right)\right] r_r \qquad (1)$$

$$r_r = x_r + jy_r, \quad j = \sqrt{-1}, \quad |r_r| = \sqrt{x_r^2 + y_r^2}$$

where $M_f$ is fluid inertia effect, D is fluid film radial damping, and $K_0$ and $K_B$ are linear and nonlinear parts of the fluid film radial stiffness, respectively. The nonlinearity here is considered in the general form of a continuous function of the rotor lateral displacement $|r_r|$ limited by the radial clearance, *c*. In general, the fluid film stiffness is an increasing function of eccentricity. Eq. 1 yields the formal definition of $\lambda\Omega$, which can be found in Eq. (1); it is an *angular velocity at which the fluid force rotates*. Based on circumferential flow pattern analysis [10] $\lambda$ is called *fluid circumferential average velocity ratio*. The transformation $r_r = re^{j\lambda\Omega t}$ of Eq. (1) into the stationary coordinates *x, y* yields:

$$-F = -F_r e^{j\lambda\Omega t} = M_f\left(\ddot{r} - 2j\lambda\Omega\dot{r} - \lambda^2\Omega^2 r\right) + \qquad (2)$$

$$+ D\left(\dot{r} - j\lambda\Omega r\right) + \left[K_0 + K_B\left(|r|\right)\right] r, \; r = x + jy$$

where *F* is the fluid force in stationary coordinates. In this format, the fluid force can be directly introduced into the classical rotor model. This force is acting on the rotor. In Eq. (2), *x* and *y* are lateral orthogonal displacements of the rotor (at the fluid force axial location) described in the stationary coordinate system. From the rotor stability standpoint, the most important component of the fluid force (2) is the tangential component, $jD\lambda\Omega r$. (The "*j*" indicates that this term is perpendicular to the radial direction, *r*). The coefficient $D\lambda\Omega$ is known as the "cross stiffness" term. In the model (2), this "coefficient" is obtained based on flow average velocity consideration, and with predominantly circumferential flow, it results from the damping force rotation. It is, therefore, a product of well-defined physical parameters D, $\lambda$ and $\Omega$.

The fluid force model (2) has been identified through extensive modal testing [4-6]. The simplified fluid force model in which $\lambda = 0.5$ has been mentioned in engineering literature since the early 1960s [11, 12]. However, this is only a very rough approximation. With an assumed constant value of $\lambda$, the model cannot reflect important features of the fluid force. The ratio, $\lambda$, is actually not a constant coefficient, but a function of rotor eccentricity (Figure 3), rotative speed, and a function of the fluid parameters and flow pattern. The flow pattern can easily be modified by bearing or seal fluid inlet/outlet conditions, such as preswirls, geometry of operating "cylinder" surfaces (e.g., multi-lobe bearings, labyrinth seals), swirl brakes, fluid antiswirl injections (Figure 4 [13, 14]), etc. The modifications of the fluid flow pattern, from a pure concentric rotor rotation-induced circumferential pattern into a predominantly axial pattern, reduces the value of $\lambda$ and improves the rotor stability. In the next section, it will be shown how $\lambda$ is related to the stability of rotor/bearing/seal systems.

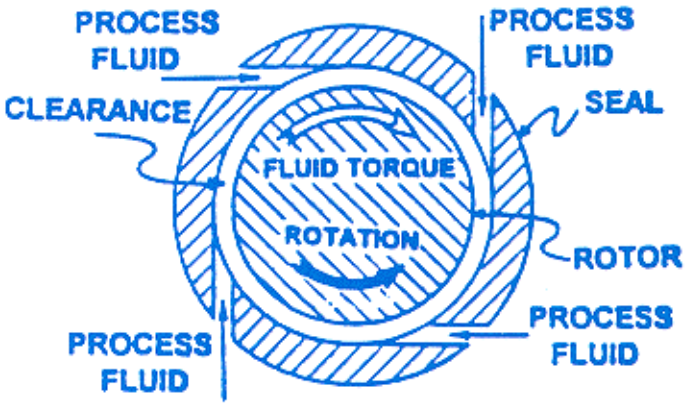


**Figure 4**

**Antiswirl injection principle: fluid injected tangentially to the seal in the direction opposite to rotation produces fluid torque which reduces rotation-generated fluid circumfernential average velocity, $\lambda\Omega$ [13, 14].**

## Rotor/seal rotor/bearing and models

The model of the rotor system with the assumption on system isotropy, limiting considerations to the first lateral mode, and using Eq. (2) (with fluid inertia neglected for clarity), is as follows (Figure 5):

$$M\ddot{r}_1 + D_s\dot{r}_1 + (K_1 + K_2)r_1 - K_2 r_2 = 0, \qquad (3)$$

$$r_i(t) = x_i(t) + jy_i(t), \quad i = 1,2$$

$$D(\dot{r}_2 - j\lambda\Omega r_2) + \left[K_2 + K_3 + K_0 + K_B(|r_2|)\right]r_2 - K_2 r_1 = 0$$

where M,$D_s$ are rotor modal mass and damping, respectively, $K_1$,$K_2$,$K_3$ are rotor partial modal stiffnesses for the rotor/seal model (Figure 5a); $K_B$ is the rotor supporting spring stiffness for the rotor/bearing model (Fig. 5b). $r_1$ and $r_2$ are rotor lateral displacements at the disk and at the fluid force location in the complex number format.

First the system eigenvalues will be discussed. The characteristic equation for the linear system (3) ($K_B$ =0) is as follows:

$$\left(K_1 + K_2 + sD_s + Ms^2\right)\left[D(s - j\lambda\Omega) + K_2 + K_3 + K_0\right] - K_2^2 = 0 \qquad (4)$$

where $s$ is the eigenvalue. Introducing the complex eigenvalue $\omega$ by $s = j\omega$, Eq. (4) can be transformed into the following approximate form:

$$\omega \approx \lambda\Omega\left\{1 - \frac{D_s K_2^2}{D\left[(K_1 + K_2 - M\lambda^2\Omega^2)^2 + D_s^2\lambda^2\Omega^2\right]}\right\} + \qquad (5)$$

$$+\frac{j}{D}\left(K_0 + K_3 + K_2\frac{K_1 - M\lambda^2\Omega^2}{K_1 + K_2 - M\lambda^2\Omega^2}\right)$$

where on the right side of Eq. (5) $\omega$ was replaced by $\lambda\Omega$, (the zero-th approximation), and some terms with $D_s$ were omitted. The real part of Eq. (5) represents the first approximation to one of the system natural frequencies. Since the second term of the real part of (5) is proportional to the rotor damping,$D_s$, its value is small. Therefore, this frequency is approximately $\lambda\Omega$. The imaginary part of Eq. (5), when equalized to zero, provides the instability threshold $\Omega_{th}$:

$$\Omega_{th} \approx \frac{1}{\lambda}\sqrt{\frac{1}{M}\left[K_1 + \frac{K_2(K_0 + K_3)}{K_2 + (K_0 + K_3)}\right]} \qquad (6)$$

The last expression under the radical in Eq. (6) represents two stiffnesses, $K_2$ and $K_0$+$K_3$ in series. Therefore, it results in a stiffness lower than either of the components results. In the rotor/seal case (Figure 5a), this produces a value which may significantly contribute to $K_1$. As a result, the instability threshold (6) becomes relatively high, often as high as twice the first natural frequency of the system. In this range, the fluid whirl vibrations do not exist, and the resulting self-excited vibrations are of a whip type. This is not the case for the rotor/bearing system. The stiffness of the supporting springs, $K_3$, if ever installed, is usually small. The fluid film stiffness is even lower, so the last term in Eq. (6) can practically be neglected in comparison to $K_1$. The rotor/bearing system instability threshold reduces, therefore, to $\Omega_{th} \approx \sqrt{K_1 M}\ \lambda$. This value may be much lower than the high eccentricity first balance resonance (as shown in Figure 2). At such a low speed, the post-instability threshold self-excited vibrations are fluid whirl. Note that the instability threshold (6) is inversely proportional to $\lambda$. A lower $\lambda$ produces a higher instability onset. Here, therefore, is where one must look for the system stability improvements. Antiswirl injections [13, 14] are an excellent way to increase stability. Note, also, that the onset of instability does not depend on the amount of fluid damping, $D$.

The remaining two eigenvalues from Eq.(5) provide two more natural frequencies of the system. The latter are close to the natural frequency of the forward and backward bending modes of the rotor itself. Using Eq. (4), it can be shown that, for the positive complex eigenvalue with the rotor natural frequency $\omega_{n1} \approx \sqrt{(K_1 + K_2)/M}$, the imaginary part reaches zero at a certain speed. This corresponds to the whip cessation ([17]; see Figure 6).

The rotor limit cycle of self-excited lateral vibrations of whirl or whip, which occurs after the onset of instability,(6) can be found by solving Eqs. (3). The transition from a stable rotor, $r_1$=$r_2$=0 into the limit cycle is not considered here.

$$r_1 = A_1 e^{j(\omega t + \alpha)}, \quad r_2 = A_2 e^{j\omega t} \qquad (7)$$

where $A_1$ and $A_2$ are amplitudes of the rotor disk and journal limit cycle circular precession, $\omega$, is the frequency of the whirl or whip, and $\alpha$ is the relative phase angle between the

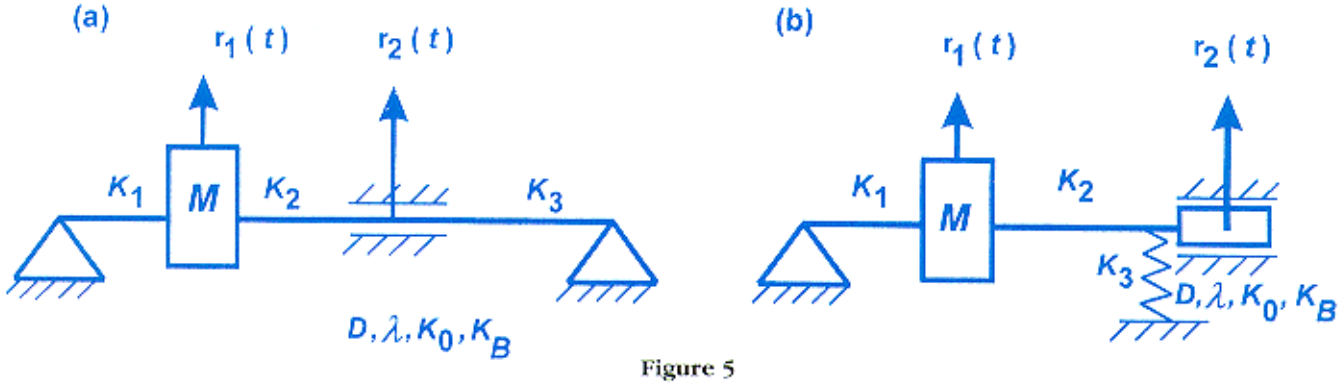


**Figure 5**
**Rotor/seal (a) and rotor bearing (b) models.**

disk and journal (or rotor at seal location) vibrations. These parameters can be calculated from two algebraic equations obtained by substituting Eqs.(7) into(3). After some transformations, they are as follows:

$$(K_1 + K_2 - M\omega^2 + jD_s\omega)\left[jD(\omega - \lambda\Omega) + \right. \\ \left. + K_2 + K_3 + K_0 + K_B(A_2)\right] - K_2^2 = 0 \quad (8)$$

$$A_1 e^{j\alpha} = K_2 A_2 \Big/ \left(K_1 + K_2 - M\omega^2 + jD_s\omega\right) \quad (9)$$

From Eq. (8), the frequency, $\omega$, and amplitude, $A_2$, can be calculated. Eq. (9) provides $A_1$ and $\alpha$. Eq. (8) has virtually the same format as the characteristic equation (4) with $s=j\omega$, except for an additional nonlinear term $K_B(A_2)$. (Note that with the assumed general form of the fluid film radial stiffness nonlinearity, this function now becomes the algebraic function of the amplitude, $A_2$.) The frequency of the self-excited vibrations, $\omega$, will be close to one of the natural frequencies calculated from Eq. (4). Therefore, it will be either close to $\lambda\Omega$ (for whirl) or the rotor high eccentricity natural frequency of the bending mode, $\omega_n$ (for whip).

Eq. (9) provides a clue which allows identification of the axial location of the instability source of whirling or whipping in the machine train rotor. The phase, $\alpha$, is the relative phase between the whirl or whip vibration at the instability source and the other portion of the rotor. Since $\omega$, the frequency of fluid whirl or whip, is generally lower than $\omega_n$, the angle $\alpha$ is, therefore, negative. Therefore, the disk self-excited vibration lags the journal one, where the instability occurs. By measuring the phases of the filtered whirl or whip vibrations at two or more axial locations along the rotor, the instability source can, therefore, be pinpointed. This method is now successfully used in the industry [15]. When the rotor is at whip, the frequency, $\omega$, is close to $\omega_n$ and $\alpha=-90°$. The rotor mode at whip is, therefore, a "corkscrew" shape.

## Higher modes of fluid whirl and whip

Extensive experiments, including modal perturbation testing and the identification of rotor system modal parameters, have produced more accurate models of fluid-induced forces in seals and lightly-loaded bearings. These experiments have also led to the discovery and explanation of undocumented earlier phenomena, such as higher-mode fluid whirl (Figure 6) and higher mode whip self-excited vibrations [16-18].

## Physical factors affecting fluid whirl and whip

In this article, we will discuss several physical factors that influence the fluid-induced, self-excited vibrations (whirl and whip).

### *Radial Sideload Force*

A rotor unbalance, generating the radial rotating force, may temporarily stabilize the rotor by suppressing the whirl during its run-up or coastdown in the balance resonance speed range. The application of higher unbalance is not, however, an advised cure to avoid fluid-induced vibrations. A constant, rotative speed independent, radial sideload force applied to the rotor is more effective. This force can be generated by rotor alignment, by process fluid distortion in fluid-handling machines, or finally, by gravity, when the journal side of the horizontal rotor is made heavier[1]. In the rotor rig (Figure 1), the radial force can be controlled by supporting springs. The radial sideload forces made the journal move to a higher eccentricity inside the bearing. At the higher eccentricity, two positive factors operate: a larger fluid film stiffness and a lower $\lambda$ (see Figure 3), as the predominantly circumferential flow pattern changes. By increasing the direct bearing stiffness, the mechanical resonance frequency is increased. By lowering $\lambda$, the fluid-induced resonance frequency is decreased. Therefore, higher rotor eccentricity increases the margin of stability by separating the mechanical resonance and fluid-induced resonance. Both these factors affect the stability threshold (6): An increase of $K_0$ and a decrease of $\lambda$ result in higher $\Omega_{th}$, hopefully above the operating speed range.

A word of caution should be added here regarding the applied radial force magnitude: a small amount of the force may sufficiently stabilize the rotor (a "friendly sideload"). Too much force would worsen bearing lubrication conditions and impose a stress on the rotor, which, ultimately, can lead to cracks and the rotor breakage (an "unfriendly sideload").

### *Rotor Configuration*

Traditionally the cure for fluid-induced instabilities was sought in redesigning the rotor by making it shorter, fatter, and more rigid. This results in a higher first natural frequency, and in a higher instability threshold (6), as $K_1$ and $K_2$ increase. Analyzing, Eq. (6), you will note, that for the rotor bearing system (Fig. 5b), the major stiffness component of the instability threshold is $K_1$. For a constant total stiffness $K_1+K_2$ and a constant $\lambda$, a small $K_1$ means that the rotor mass is very close to the journal. It also means that the instability threshold occurs at lower rotative speed. A high $K_1$ improves the stability situation. An immediate conclusion is to move the major mass of the rotor away from the fluid-lubricated bearing and maintain required journal eccentricity at the bearing using other means than gravity. This fact was confirmed experimentally [3].

### *Bearing Geometry*

For a long time, bearing designers have known that a plain cylindrical bearing is the worst design for rotor stability. Improvements were achieved by modifying bearing

[1]Note, however, that making the rotor "heavier" does not mean that an improvement is achieved. From one aspect, this is due to the existence of other radial forces, such as supporting spring forces (if the springs exist) controlling journal eccentricity. From another aspect, it is due to the role of rotor mass. Note in Eq (6) the higher mass $M$ is , the *lower* instability threshold is!

geometry. Elliptical, lemon-shaped bearings, bearings with grooves and lobes, and bearings with mobile parts, such as a tilting pad bearings, are generally more stable than plain cylindrical bearings. These improved features are associated with changes in the circumferential flow, which, in all these improved designs, has a *lower strength*, due to boundary conditions, than in cylindrical bearings. Therefore, $\lambda$ is smaller, and the instability threshold is (6) higher. The decision to replace machine bearings with a more stable design should be, however, justified by the analysis that the bearings (not the main flow) *are* the machine problems.

### *Rotating Bearing Around a Stationary Post. Rough Journal Surface*

Interesting experimental results were obtained when the bearing shell was mounted on the shaft, and the journal was simulated by a stationary post. When maintaining the same geometric dimensions and lubrication pattern as in the traditional rotor/bearing system (Figure 1), the whirl frequency was 0.51Ω (as opposed to 0.47Ω for the regular bearing). Therefore, the increased linear velocity, $R$ (R=radius) of the outer rotating surface, which drags the fluid into rotational motion, increased the fluid circumferential average velocity [17]. In other experiments, a steel journal became rusty, due to the use of an inappropriate lubricant. Its acquired surface roughness and higher friction caused an increase of the fluid circumferential average velocity ratio and, consequently, an increase in whirl frequency from 0.47 Ω to 0.49Ω.

### *Fluid Pressure*

For partially lubricated bearings ("180° bearings"), the lubricant pressure should be controlled. For example, it should be lower than 20 psi (958 Pa), as a higher pressure may change the lubrication pattern from partial to full. This will create a fully-developed circumferential flow, and more favorable conditions for whirl and whip. In the case of full lubrication, increased fluid pressure, which proportionally increases the fluid radial stiffness, is beneficial for stability. Externally-pressurized ("hydrostatic") bearings are well-known for their excellent stability features. In seals, a higher leakage flow may lower the circumferential flow ($\lambda$), while deteriorating machine efficiency, may prevent fluid-induced vibrations.

### *Fluid Temperature*

Traditionally, the first quick-fix tried when a machine rotor started whirling or whipping was to change bearing lubricant temperature. Oil temperature changes were easy to accomplish, being external to the online operating machine. The direction of temperature changes was, however, more difficult to determine. In approximately 40% of cases, cooling the lubricant resulted in rotor stabilization. In approximately 30% of cases, heating stabilized the rotor. In the remaining cases, this fix was ineffective. Heating or cooling the lubricant mainly affects its viscosity, decreasing or increasing the fluid radial damping, $D$. This equally affects the stabilizing agent( in Eqs. (3)) and the instability driving tangential force, $D\lambda\Omega r$. Therefore, the result cannot be predicted, unless the instability threshold versus lubricant temperature is analyzed separately. This relationship is virtually nonlinear. In some cases, an increase of temperature and lower oil viscosity may also affect fluid film stiffness, which moves the journal to higher eccentricity.

Heating lubricant in only one bearing may bring some

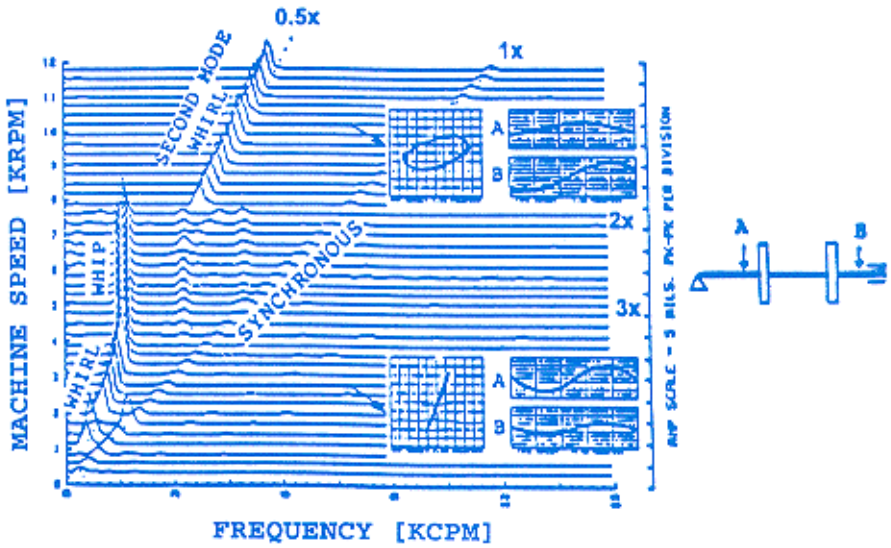


Figure 6

**Spectrum cascade of rotor vertical vibrations measured by transducer B with timebase waveforms and "orbits" produced by inboard and outboard transducers A and B at rotative speeds 2 krpm and 10.2 krpm. The "orbits" show that during whirl of the first mode, the rotor vibrates in phase, behaving as a rigid body, while during the second mode whirl the rotor ends are about 90° out of phase [15].**

additional positive effects. Due to thermal expansion, the rotor alignment state can be positively affected, providing a friendly sideload. In general, however, you shouldn't expect to bring about a long-lasting cure for whirl, and especially whip vibrations, by changing the lubricant temperature.

One more caution regarding lubricant temperature changes may be useful. A higher temperature may increase bearing clearance, which makes the bearing more prone to instability. It may also affect the readings of the proximity transducer, if its scale factor is sensitive to temperature changes.

### *Antiswirl Injections*

Fluid antiswirl injections made tangentially to the seals or bearings in the direction opposite to rotation are by far most efficient way to stabilize a rotor [13, 14]. This technique may be used in a passive or an active control mode (Figure 4) [14].

## Formal derivation of fluid forces

The formal derivation of fluid dynamic forces was based on an assumption of a short cylindrical bearing or seal, pressurized at the ends, lubricated by an incompressible fluid with fully developed, laminar circumferential flow [19]. A new solution of the Reynolds Equation was obtained in the form of an infinite series. When calculating fluid forces, stresses (not pressures!) were integrated over the displaced rotor surface (not the bearing surface!). Fluid forces in the rotor/bearing (or seal) system were then obtained assuming rotor rotation and precession at an eccentric position inside the bearing (or seal). The equations allow for extracting the elements of the fluid force (1).

## Closing remarks

This article summarizes the results of experiments on fluid-induced rotor self-excited vibrations, whirl and whip. A simple mathematical model of the fluid force at low to medium eccentricities, which was identified through modal perturbation testing [4-6] adequately predicts the rotor dynamic behavior. The rotor/bearing/seal model can also be extended to include other pertinent factors, such as fluid inertia, fluid radial stiffness, damping anisotropy and damping nonlinearity [2, 6], rotor lateral nonsymmetry, and more rotor modes. The key issue here is to adopt the multi-mode system (elastic solid body plus fluid) approach in modeling. The rotor self-excited whirl or whip vibrations can occur at any mode, acquiring a frequency corresponding to the system natural frequencies.■

## References:


1. Poritsky, H., Contribution to the Theory of Oil Whip, *Trans. of the ASME*, No. 75, 1953.
2. Muszynska, A., Whirl and Whip – Rotor/Bearing Stability Problems, *Journal of Sound and Vibration*, v. 110, No. 3, 1986, pp. 443-462.
3. Bently, D. E., Muszynska, A., Perturbation Study of a Rotor/Bearing System: Identification of the Oil Whirl and Oil Whip Resonances, *ASME*, Paper 85-DET-142, Cincinnati, OH, 1985.
4. Muszynska, A., Modal Testing or Rotor/Bearing Systems, *The International Journal of Analytical and Experimental Modal Analysis*, v. 1, No. 3, pp. 15-34, 1986.
5. Muszynska, A., Modal Testing of Rotors With Fluid Interaction, *International Journal of Rotating Machinery, v. 1, No. 2, 1995.*
6. Muszynska, A., Bently, D. E., Frequency Swept Rotating Input Perturbation Techniques and Identification of the Fluid Force Models in rotor/Bearing/Seal Systems and Fluid Handling Machines *Journal of Sound and Vibration*, v. 143, No. 1, 1990, pp. 103-124.
7. Muszynska, A., Improvements in Lightly Loaded Rotor/Bearing and Rotor/Seal Models, *ASME Journal of Vib., Ac., Stress & Rel. in Des.*, v. 110, No. 2, 1988.
8. Muszynska, A., Fluid Dynamic Force Model for Rotors With Seals or Lightly Loaded Bearings, *Orbit*, v. 15, No. 4, December 1994.
9. Bently, D. E., Rotordynamic Aspects of Rotating Stall in Radial Compressors, ISROMAC-5, Maui, HI, 1994.
10. Tam, L. T., Przekwas, A. J., Muszynska, A., Hendricks, R. C., Braun, M. J., Mullen, R. L., Numerical and Analytical Study of Fluid Dynamic Forces in Seals and Bearings, *ASME Journ. of Vib., Ac., Stress & Rel. in Des.*, v. 110, No. 3, 1988.
11. Bolotin, V. V., The Dynamic Stability of Elastic Systems (translated from Russian), Holden-Day, San Francisco, CA, 1964.
12. Black, H. F., Effects of Hydraulic Forces in Annular Pressures Seals on the Vibrations of Centrifugal Pump Rotors, *Journal of Mechanical Engineering Science II*, No. 2, 1969.
13. Bently, D. E., Muszynska, A., Anti-Swirl Arrangements Prevent Rotor/Seal Instability, *ASME Journ. of Vib., Ac., Stress & Rel. in Des.*, v. 111, No. 2, April 1989, pp. 156-162.
14. Muszynska, A., Franklin, W. D., Bently, D. E., Rotor Active "Anti-Swirl" Control, *ASME Journ. of Vib., Ac., Stress & Rel. in Des.*, v. 110, No. 2, 1988.
15. Bently, D. E., Bosmans, R. E., A Method to Locate the Source of a Fluid-Induced Instability Along the Rotor, *ISROMAC-3*, Honolulu, HI, 1990.
16. Muszynska, A., Multi-Mode Whirl and Whip in Rotor/Bearing Systems. Dynamics of Rotating Machinery, *ISROMAC-2*, v. 2, Hemisphere Publishing Corporation, Honolulu, HI, 1988.
17. Muszynska, A., The Role of Flow-Related Tangential Forces in Rotor/Bearing/Seal System Stability, *ISROMAC-3*, Honolulu, HI, 1990.
18. Muszynska, A., Grant, J. W., Stability and Instability of a Two-Mode Rotor Supported by Two Fluid-Lubricated Bearings, *ASME Journ. of Vib.and Acou.*, v. 113, No. 3, 1991.
19. Petchenev, A., Goldman, P., Muszynska, A., Bently, D. E., Analytical Study on the Fluid Journal Bearing/Seal/Rotor System, *The Joint ASME & JSME, Fluids Eng., Annual Conf.*, Hilton Head Island, SC, 1995.


## Eccentricity ratio

Eccentricity ratio, either dynamic (instantaneous) or average, is a dimensionless quantity representing the radial position of the shaft within the clearance. It is obtained by dividing the distance between the shaft centerline and the bearing (or seal) centerline by the radial clearance. Values of eccentricity ratio range from 0 (the shaft is centered in the clearance) to 1.0 (the shaft is touching the bearing or seal).■